https://doi.org/10.5194/essd-2024-365
Preprint. Discussion started: 20 September 2024

Open Access Earth System Science Data Discussions

A consistent regional dataset of dissolved oxygen in the Western Mediterranean Sea (2004-2023): O2WMED

Malek Belgacem[1], Katrin Schroeder[1], Siv K. Lauvset[2], Marta Álvarez[3], Jacopo Chiggiato[1], Mireno Borghini[4], Carolina Cantoni[5], Tiziana Ciuffardi[6], Stefania Sparnocchia[5]

[1] CNR-ISMAR, Arsenale Tesa 104, Castello 2737/F, 30122 Venice, Italy
[2] NORCE Norwegian Research Centre, Bjerknes Centre for Climate Research, Bergen, Norway
[3] Instituto Español de Oceanografía, IEO-CSIC, A Coruña, Spain
[4] CNR-ISMAR, Via Santa Teresa, Pozzuolo di Lerici, 19032 La Spezia, Italy
[5] CNR-ISMAR, Area Science Park, Basovizza, 34149 Trieste, Italy
[6] Department of Sustainability, St Teresa Marine Environment Research Centre, ENEA, Pozzuolo di Lerici, 19032 La Spezia, Italy

Correspondence to: Malek Belgacem (malek.belgacem@ve.ismar.cnr.it)

Abstract. A new dataset from oceanographic cruises in the Western Mediterranean Sea (WMED) was compiled to integrate the previously published regional data product CNR-DIN-WMED about dissolved inorganic nutrients (https://doi.org/10.1594/PANGAEA.904172, Belgacem et al., 2019, 2020). The Mediterranean region is experiencing rapid changes, necessitating high-quality and reliable datasets. However, the scarcity of the in-situ observations hinders the understanding of these changes and their impact on biogeochemical cycles. Dissolved oxygen is a vital component of marine ecosystems and plays a fundamental role in governing nutrient and carbon cycles, underscoring the need for accurate and reliable data. To address this, a high resolution, regional-scale data product was developed to understand decadal variability and spatial/temporal patterns of the ventilation process in the WMED. This study presents an extensive collection of unpublished dissolved oxygen data from continuous sensors collected between 2004 and 2023, along with a description of the quality assurance procedures. The quality assurance process involves calibration of CTD measurements against Winkler analyses and the comparison of deep observations with reference datasets, using the crossover analysis. The resulting data product O2WMED can be used as reference for assessing oxygen sensors mounted on biogeochemical Argo (BGC-Argo) floats or Gliders and for regional model validation.

Data coverage

Coverage: 44∘ N–35∘ S, 6∘ W–14° E
Location name: western Mediterranean Sea
Date/time start: October 2004
Date/time end: April 2023

1 Introduction

Oxygen plays a crucial role as a fundamental oceanic variable. The ocean produces about 50% of the earth's oxygen, which is crucial for the atmospheric oxygen inventory (Grégoire et al. 2023). The ocean's oxygen levels are highly susceptible to changes, through

https://doi.org/10.5194/essd-2024-365
Preprint. Discussion started: 20 September 2024

Open Access Earth System Science Data Discussions

Photosynthesis occurs in the surface layer, where oxygen is produced by primary producers, leading to high surface productivity and cause the sinking of organic matter which stimulate oxygen consumption in the deep sea, leading to the creation of the Oxygen Minimum zones (OMZs). The OMZs have become more frequent in the last decade.

Increased degradation of organic matter in the deep ocean intensifies dissolved oxygen consumption. Warming conditions contribute to the heightened stratification periods and an intensification of the pycnocline, impacting biological activity and thus dissolved oxygen consumption. Additionally, factors such as denitrification and the extension of the OMZs can influence the nitrogen: phosphorus (N:P) ratio and the levels of primary productivity. Warming seawater, increased stratification and higher CO_2 levels have reshaped community distribution and ecosystem composition, resulting in decreased dissolved oxygen levels (Grégoire et al., 2023).

The decline in oxygen can be attributed to lower solubility rates due to warming and increased water column stratification, reducing the downward diffusion and mixing of well-oxygenated surface waters towards deeper layers. Such changes in oxygen concentration can trigger variations in the biological loop and the distribution of biogeochemical tracers, which have significant implications for marine ecosystems, particularly in vulnerable hotspots.

The Mediterranean Sea has been notably affected by these changes, especially in the past decade, characterized by frequent marine heat waves episodes (Marullo et al., 2023; Martinez et al., 2023; Pastor and Khodayar et al., 2023). Rising temperatures can disturb the distribution and availability of dissolved oxygen in seawater (Reale et al., 2022; Alvaréz et al. 2023). The region's enclosed nature and its peculiar thermohaline circulation further complicates the understanding of oxygen dynamics (Powley et al., 2016). Observational efforts, such as the Medar/Medatlas project (Fichaut et al., 2003), the MED-SHIP transects (https://www.go-ship.org/) (Schroeder et al., 2015), have provided valuable insights, but uncertainties remain regarding the long-term impacts of deoxygenation and acidification on Mediterranean marine ecosystems (Coppola et al., 2018).

To address these pressing issues, a compilation of oxygen observations collected by the Italian National Research Council (CNR), between 2004 and 2023 in the Western Mediterranean Sea (WMED) is documented. This effort aims to provide reliable measurements of dissolved oxygen, thereby enhancing our understanding of biogeochemical cycling and ventilation in the region. The purpose of this paper is to describe the oxygen data collected by the CNR and report the quality control procedure to justify the recommended corrections applied to the oxygen data.

2 Dissolved oxygen data collection

2.1 The CNR data collection

The **O**xygen in the **WMED** (O2WMED) dataset contains 1,382 CTD oxygen profile. In Figure 1, the spatial distribution of CTD profiles is depicted, highlighting the extensive coverage across the Northern Western Mediterranean (WMED) and key hydrographic transects.

Measures are concentrated in the eastern part of the WMED: the subregions of the Ligurian sea, Tyrrhenian and along the Tunisia-Sicily-Sardinia area. Spanning two decades from 2004 to 2023, the dataset exhibits robust temporal coverage, particularly between 2004 and 2015 (see Fig.2a). In particular, the years 2005, 2006, 2010, and 2012 stand out with the highest number of CTD stations, coinciding with years that included monthly surveys,

https://doi.org/10.5194/essd-2024-365
Preprint. Discussion started: 20 September 2024

indicating a more frequent repeat frequency (see Fig. 2). While reasonable temporal coverage is observed between 2004 and 2015 (except for 2014), the availability of stations diminishes between 2016 and 2023.

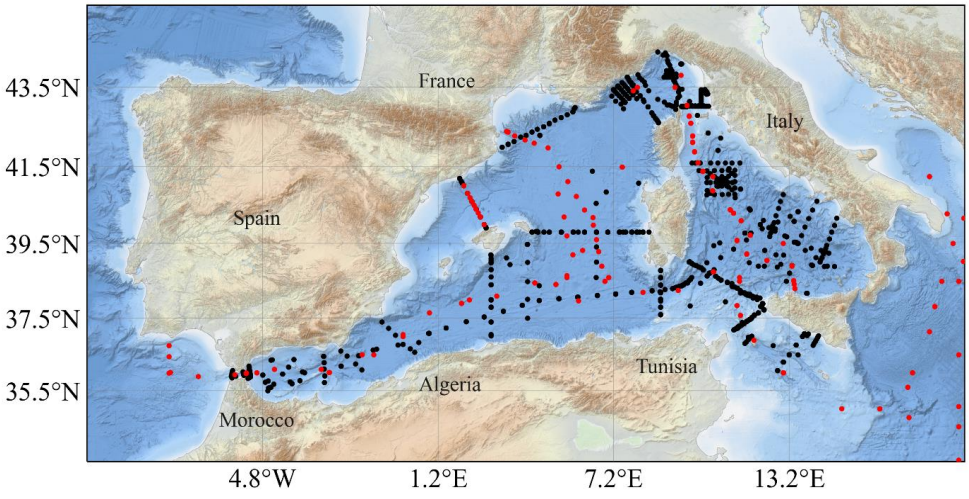

Figure 1. Spatial distribution of cruise stations with CTD oxygen data (black dots) in the O2WMED CNR dataset across the WMED. The red markers indicate stations from selected reference cruises.

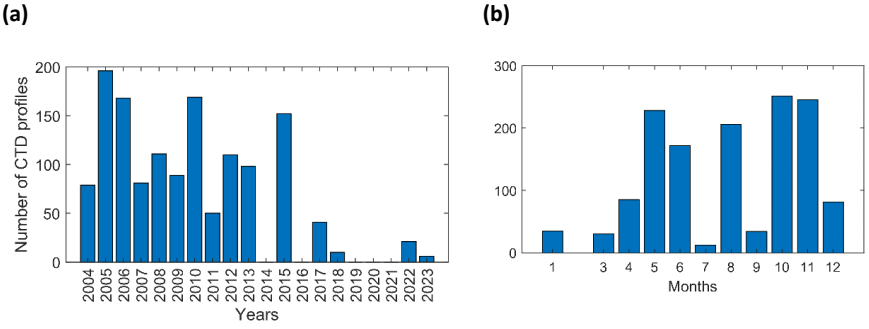

Figure 2. Temporal distribution of CTD profiles with oxygen in the O2WMED CNR dataset: A. annual distribution and B. monthly distribution.

Data included in the dataset (Table 1) were routinely calibrated against Winkler measurements following Grasshoff et al. (1983) and Langdon (2010). Discrete samples were used to calibrate the CTD sensor to correct any potential bias and adjust drift in the SBE 43 oxygen sensor following Janzen et al. (2007) and Uchida et al. (2010). Details regarding the post-calibration against Winkler observation can be found in the supplementary materials (Table S1).

https://doi.org/10.5194/essd-2024-365
Preprint. Discussion started: 20 September 2024

Open Access Earth System Science Data Discussions

Table 1. Cruise summary table listed with number of stations. Refer to Belgacem et al. (2020) and Ribotti et al. (2022) for cruise metadata.

Cruise ID no.	Common name	EXPOCODE	Date Start/End	CTD profiles	Maximum bottom depth (m)
2	MEDGOOS9	48UR20041006	6 - 25 OCT 2004	79	3668
3	MEDOCC05/ MFSTEP2	48UR20050412	24 APR - 16 MAY 2005	160	3657
5	MEDGOOS11	48UR20051116	16 NOV - 3 DEC 2005	36	3494
6	MEDOCC06	48UR20060608	8 JUN - 3 JUL 2006	127	2882
8	MEDGOOS13/MEDBIO06	48UR20060928	28 SEP - 8 NOV 2006	41	4137
9	MEDOCC07	48UR20071005	5 - 29 OCT 2007	81	3497
10	SESAMEIt4 KM3 or SESAME_KM3	48UR20080318	18 MAR - 7 APR 2008	27	3510
11	SESAMEIT5 (Sesame KM3 September 2008)	48UR20080905	5 - 16 SEP 2008	24	3450
12	MEDCO08	48UR20081103	3 - 24 NOV 2008	60	3443
13	TYRRMOUNTS	48UR20090508	8 MAY - 3 JUN 2009	89	3509
14	BIOFUN010	48UR20100430	30 APR - 17 MAY 2010	29	3541
15	VENUS1	48UR20100731	31 JUL - 25 AUG 2010	116	3649
16	BONSIC2010	48UR20101123	23 NOV - 9 DEC 2010	24	3539
17	EUROFLEET11	48UR20110421	21 APR - 8 MAY 2011	32	3541
18	BONIFACIO2011	48UR20111109	9 - 23 NOV 2011	18	3542
20	ICHNUSSA12	48UR20120111	11 - 27 JAN 2012	35	3552
21	EUROFLEET2012	48UR20121108	8 - 26 NOV 2012	75	3554
211	VENUS 2	48UR20130604	4 - 25 JUN 2013	59	3539
22	ICHNUSSA13	48UR20131015	15 - 29 OCT 2013	40	3542
222	ICHNUSSA15	48QL20151123	23 NOV - 14 DEC 2015	62	3633
23	OCEANCERTAIN15	48QL20150804	4 - 18 AUG 2015	90	3514
24	ICHNUSSA17/INFRAOCE17	48QL20171023	23 OCT- 28 NOV 2017	41	3537
25	ICHNUSSA/JERICO18	48DP20180918	18-25 SEP 2018	10	525
27	JERICO-II-2022	48DP20221015	15- 25 OCT 2022	21	1004
28	JERICO-III-EurogoShip-2023	48DP20230324	24 MAR - 09 APR 2023	6	909

The vertical distribution of dissolved Oxygen in the WMED exhibits a distinct pattern across different depth layers as illustrated in the vertical profiles shown in Fig.3(a). These profiles, which span ten subregions, provide a comprehensive view of spatial coverage, considering the depth component in conjunction with the reference dataset.

Broadly speaking, profiles reveal a general trend of high concentrations in both the upper and bottom layers, with an intermediate oxygen minimum layer, typically observed between 400 and 600 meters (Mavropoulou et al., 2020). At greater depths, subregions exhibit distinct behaviors. The dissimilarities in the vertical distribution highlight regional variations, influenced by factors such as circulation patterns, biological activity, and the unique physical characteristics of each region. This is particularly true for the Mediterranean, characterized by a complex circulation pattern involving inflows from the Atlantic Ocean, surface currents, and deep-water formation. Circulation patterns play a crucial role in transporting oxygen-rich or oxygen-poor water masses to different regions (Mavropoulou et al., 2020). For instance, in Figure 3a the DF2-Gulf of Lion, oxygen-rich waters reach the deep WMED by means of winter deep convection.

https://doi.org/10.5194/essd-2024-365
Preprint. Discussion started: 20 September 2024

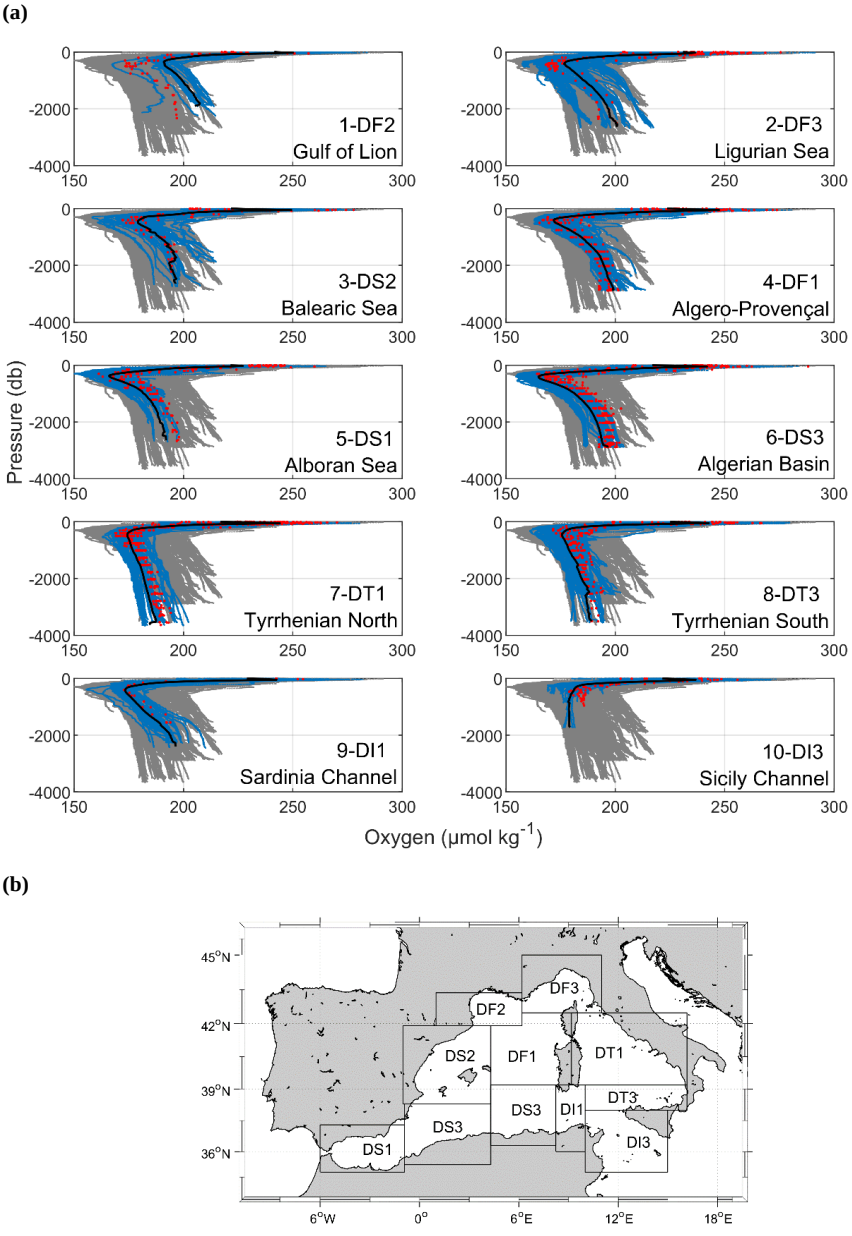

Figure 3. (a) Vertical profiles of oxygen distribution for the entire WMED in grey, from the original dataset after the initial quality control (1st QC). The blue represents the vertical distribution within each subregion (refer to Table S1). The black lines denote the mean profile of each subregion over the entire study period. The red lines represent the reference data for each region. (b) Geographical map of the WMED indicating the geographical limits from MEDAR/Medatlas sub-regions (defined in Table S1). Adapted from Manca et al. (2004).

2.2 Reference data

The previously described CNR collection data is compared to deep water data collected in the same area (details are in section 3.2).

https://doi.org/10.5194/essd-2024-365
Preprint. Discussion started: 20 September 2024

A total of six cruises have been identified (see Table 2) with documented high-quality dataset (Figure 4), collected in the Mediterranean Sea through international projects. Defined as "reference cruises," they adhere to the recommendations of the World Ocean Circulation Experiment (WOCE) and the Global Ocean Ship-Based Hydrographic Investigations Program (GO-SHIP) protocols (Langdon 2010). Among these, cruises 06MT20011018 and 06MT20110405 are significant surveys, contributing to the GLODAPv2 dataset (Olsen et al., 2016), which facilitate comprehensive mapping of biogeochemical parameters.

During cruise both cruises, quality control procedures were applied to data, and minimal corrections to oxygen measurements were made, ensuring excellent data quality. Additional information regarding these cruises can be found in the work of Tanhua et al. (2013a) and Hainbucher (2012). For further details regarding these references, one can refer to the adjustment table available at https://glodap.info/ (last access: August 2024) and the work by Olsen et al. (2020).

Similarly cruises 48UR20070528 (TRANSMED II) and 29AH20140426 (HOTMIX) which are related to CARIMED (CARbon, tracer and ancillary data In the MEDsea) that aims to be an internally consistent database containing inorganic carbon data relevant for this basin (Álvarez et al., in preparation); which means that this cruise underwent rigorous quality control processes

The TALPpro cruises conducted in 2016 (Tanhua ,2019a, 2019b; Jullion, 2016) and in 2022 (Schroeder, 2022) are associated with the MedSHIP program, which follows the guidelines established by the international GO-SHIP initiative. This program is dedicated to high-quality data collection and analysis to evaluate the impacts of climate on marine environments (Schroeder et al., 2015, 2024).

Following the standards and charts of these programs, the quality of measurements obtained during these cruises has been ensured, demonstrating both precision and reliability, and thus used as reference cruises in the secondary quality control procedure described below in section 3.2.

Table 2. Overview of reference cruises utilized in the secondary quality control process with their Expocode and Identification number (ID). The data spans from 2001 to 2022.

ID	*Common name*	EXPOCODE	Date starts and end	Stations	Source	Chief scientist(s)
6	*M51/2 TRANSMED_LE*	06MT20011018	*18 Oct–11 Nov 2001*	6	GLODAPv2	Wolfgang Roether
22	*GII*	48UR20070528	*28 May–12 Jun 2007*	4	CARIMED	Maurizo Azzaro
64	*M84/3*	06MT20110405	*5–28 Apr 2011*	20	GLODAPv2	Toste Tanhua
17	*HOTMIX*	29AH20140426	*26 Apr–31 May 2014*	18	CARIMED	Javier Aristegui
27	*TAlPro-2016*	29AJ20160818	*18–28 Aug 2016*	42	MedSHIP programme	Loïc Jullion, Katrin Schroeder
28	*TAlPro-2022*	11BG20220517	17-26 May 2022	24	MedSHIP programme MedSHIP/	Katrin Schroeder

(a) (b)

https://doi.org/10.5194/essd-2024-365
Preprint. Discussion started: 20 September 2024

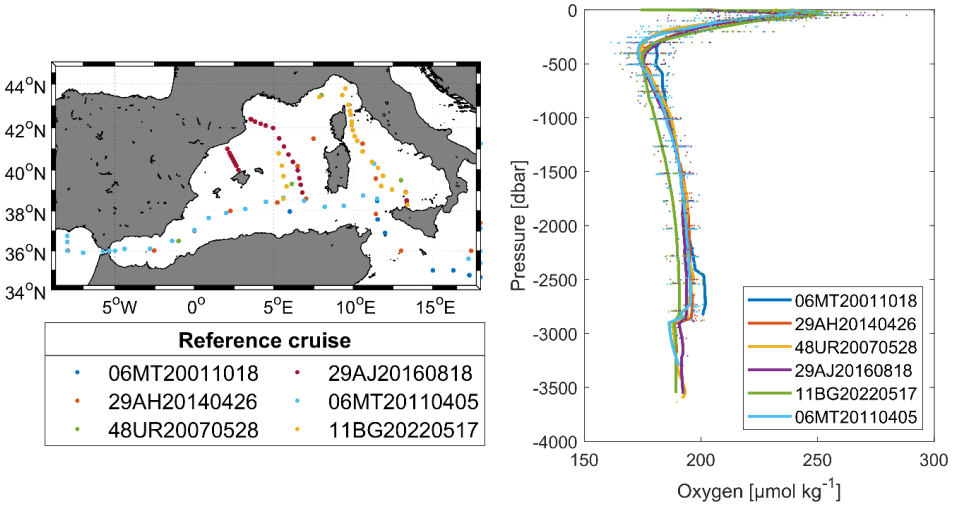

148 **Figure 4. Reference cruises: (a) Map with stations. (b) Dissolved oxygen data from Winkler measurements**
149 **and corresponding mean profile from the reference cruises.**

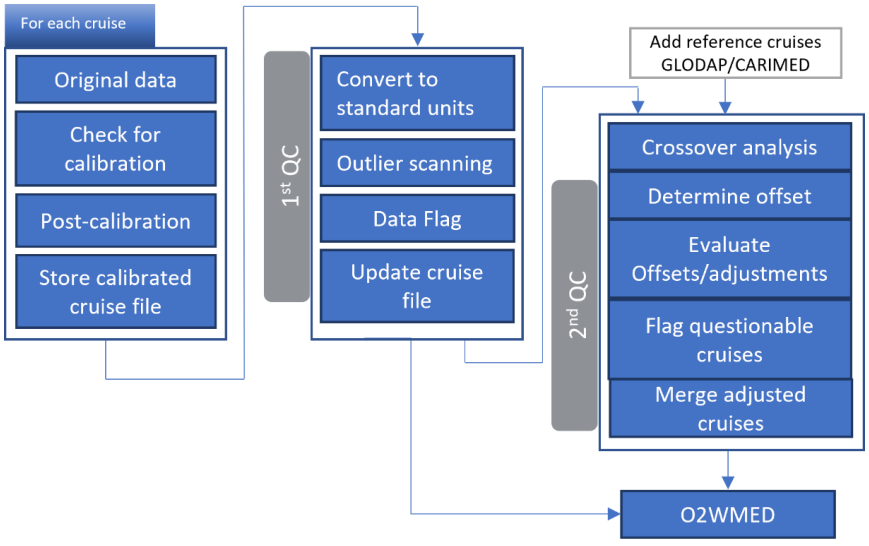

150

151 **Figure 5. Flowchart illustrating the sequential steps from calibration through primary quality control**
152 **(1stQC) to secondary quality control; refer to the text for comprehensive details.**

153

154 ## 3 Quality assurance methods

155 ### 3.1 Primary quality control of O2 CTD data

156 Following Figure 5 chart, each cruise variable was scanned for any spike before calibration. Then values were
157 converted to standard units when needed. Dissolved oxygen was converted from milliliters per liter (ml L^{-1}) to
158 micromoles per kilogram (µmol kg^{-1}) using potential density and the conversion factor 44.66 to ensure uniformity.

https://doi.org/10.5194/essd-2024-365
Preprint. Discussion started: 20 September 2024

For a thorough data integrity, each parameter was assigned a data quality flag. Initially set to 2 for acceptable values, flag 3 for questionable values and to 9 for data following WOCE.

The primary quality control (1st QC) procedure involved the identification of outlier profiles and/ or data points in each cruise. Outliers were flagged, indicating the quality of each value (refer to Table 3 in Belgacem et al., 2020). Flagging was specific to the precision of each parameter for each cruise. Property-property plots were then examined for each region, and values identified as outliers in more scatter plots were flagged as questionable (see Fig. 6).

A scatter plot depicting the oxygen distribution provided an overview, with values flagged as 3 for questionable values or 2 for accepted values. Approximately 0.19% of CTD oxygen data were considered outliers and flagged as 3. The 1st QC can be subjective, as it relies on the expertise of the individual inspecting the data.

The coefficient of variation of Oxygen profiles (CV, defined as standard deviation over mean) for each layer (surface: 0-250 db; intermediate: 250-1000 db; deep: below 1000 db) has been considered. CV in the surface layer (0-250 db, CV = 11.7%) were relatively high due large frequency variability (caused by air-sea interaction), at intermediate levels (250-1000db, CV = 4.5%), and deep layer (below 1000 db, CV =4.4%), these variabilities are reduced.

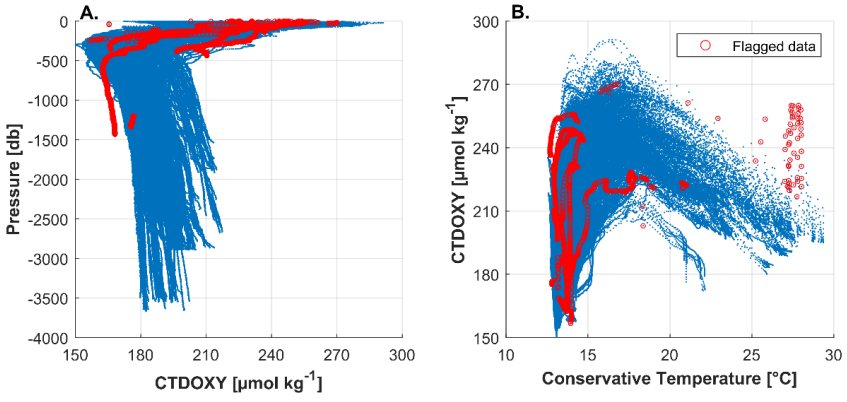

Figure 6. Summary scatter plots illustrating (A) pressure vs. Oxygen and (B) Oxygen vs. potential temperature while red circles indicate values flagged as questionable (Flag 3).

To evaluate the precision of each cruise data, adjacent profiles were compared. Standard deviations and averages were calculated for deep layers (depths greater than 1000 dbar, as shown in Table 3) to sidestep any variability associated with atmospheric forcing or mesoscale patterns.

Data with poor precision are expected to show large standard deviations, indicating significant discrepancies from nearby measurements.

Additionally, this analysis provides an overview of oxygen content in deep layers and the spatial extent of measurements for each survey. Following the subdivision of the WMED proposed by Manca et al. (2004) (see Fig. 3b and Table S1), comparison of regional averages allowed the identification of potentially suspect cruises.

https://doi.org/10.5194/essd-2024-365
Preprint. Discussion started: 20 September 2024

The standard deviation between cruises in deep layers varied between 0.5 and 7.6 µmol kg^{-1}. Overall, profiles collected in close proximity exhibit similar variability.

The lowest standard deviations were observed in data collected from the Sicily Channel (DI3) subregions during cruises no. 10, no. 11, and no. 211, indicating high data quality for these surveys.

Fifteen surveys were conducted in Sardinia Channel (DI1), all displaying similar variability. Standard deviation among cruises in this region ranged between 4 to 6.5 µmol kg^{-1}, demonstrating good agreement amid measurements.

A similar pattern was observed in the Tyrrhenian South region (DT3), which was samples by 22 cruises.

The lowest average was recorded during cruise #2, which was lower than neighboring cruises, while cruise #24 exhibited the highest average; however, the standard deviation did not show significant variation.

In the Tyrrhenian North region (DT1), eighteen cruises were conducted, with standard deviations ranging from 1.4 to 5.5. Notably, cruise no. 3 displayed a larger standard deviation of 7.5 µmol kg^{-1}.

In the Algerian basin (DS3), ten cruises were conducted, yielding standard deviations between 3.3 and 4.4 µmol kg^{-1}, similar to the findings in the Alboran Sea (DS1).

In the Algéro-Provençal region (DF1), we find data from eleven cruises, with the highest standard deviations recorded during cruises no. 3 and no. 24.

In the Balearic Sea (DS2), six cruises sampled the deep layer, all exhibiting low standard deviations, except for cruises #3 and #6, which had values of 6.1 and 7.6 µmol kg^{-1} respectively.

In the Ligurian Sea (DF3), five cruises where conducted, with cruise no.3 displaying anomalous behavior characterized by a high standard deviation and average compared to neighboring cruises, indicating that the data from cruise #3 were higher the nearby measurements.

High standard deviations suggest extensive spatial coverage, as seen in cruises no. 3, no. 6, no.12 and no.15, while low standard deviation, such as in cruise no. 11 (DI3-Sicily Channel), no. 17, and no. 8 (predominantly in DT1-Tyrrhenian North and DT3-Tyrrhenian South), suggests smaller spatial coverage.

The condition suggested by Olsen et al. (2016), which suggests that large standard deviation coupled with narrow spatial coverage implies imprecise data, was not found in our dataset.

An examination of data spread across various regions revealed that some cruises exhibited large standard deviations compared to nearby profiles. For instance, cruise no.3 (Tyrrhenian North, Balearic Sea and Ligurian Sea) had standard deviations exceeding 6.1 µmol kg^{-1}, suggesting that this cruise was less precise than the others conducted in the same region.

Comparing deep profiles provided evidence regarding data precision; uncertainties in measurements may complicate decisions about the adjustments proposed by the 2nd QC phase.

Cruises no. 25, no. 27, no. 28 did not include data below 1000 dbar; however, these datasets underwent quality checks and are included in the final dataset.

https://doi.org/10.5194/essd-2024-365
Preprint. Discussion started: 20 September 2024

Table 3. Average and standard deviation (STD) of CTD dissolved oxygen by cruise and for each region deeper than 1000 db.

Cruise ID	EXPOCODE/ region	Regional avg CTDOXY (µmol kg^{-1})	STD CTDOXY (µmol kg^{-1})
2	48UR20041006 /		**4.193**
	DS2-Balearic Sea	182.48	3.27
	DS1-Alboran Sea	181.71	3.59
	DS3-Algerian Basin	183.59	3.32
	DT1-Tyrrhenian North	177.49	3.21
	DT3-Tyrrhenian South	177.57	3.09
	DI1-Sardinia Channel	181.02	4.17
3	48UR20050412/		**9.538**
	DF2-Gulf of Lion	199.65	5.64
	DF3-Ligurian Sea	183.42	7.46
	DS2-Balearic Sea	200.67	6.15
	DF1-Algero-Provençal	197.87	5.76
	DS3-Algerian Basin	196.17	4.44
	DT1-Tyrrhenian North	191.03	4.67
	DT3-Tyrrhenian South	189.31	4.13
	DI1-Sardinia Channel	191.27	4.68
5	48UR20051116/		**3.542**
	DT1-Tyrrhenian North	191.73	2.79
	DT3-Tyrrhenian South	190.22	3.90
6	48UR20060608/		**9.76**
	DF2-Gulf of Lion	207.71	3.09
	DF3-Ligurian Sea	207.72	3.85
	DS2-Balearic Sea	195.00	7.60
	DF1-Algero-Provençal	194.82	4.95
	DS3-Algerian Basin	187.81	3.75
	DT3-Tyrrhenian South	185.06	3.49
	DI1-Sardinia Channel	188.80	4.21
8	48UR20060928/		**2.812**
	DT1-Tyrrhenian North	177.87	2.81
	DT3-Tyrrhenian South	178.15	2.80
9	48UR20071005/		**5.77**
	DF2-Gulf of Lion	185.57	1.38
	DF3-Ligurian Sea	190.87	3.37
	DS2-Balearic Sea	193.20	1.61
	DF1-Algero-Provençal	189.95	4.01
	DS3-Algerian Basin	189.55	4.16
	DT1-Tyrrhenian North	179.48	1.41
	DT3-Tyrrhenian South	180.09	2.18
	DI1-Sardinia Channel	183.39	4.15
10	48UR20080318/		**5.079**
	DT3-Tyrrhenian South	187.15	4.72
	DI3-Sicily Strait	180.18	0.72
11	48UR20080905/		**0.610**
	DI3-Sicily Channel	177.74	0.61
12	48UR20081103/		**4.81**
	DF1-Algero-Provençal	192.51	4.04
	DS1-Alboran Sea	190.61	3.17
	DS3-Algerian Basin	193.71	3.81
	DT3-Tyrrhenian South	184.63	3.14
	DI1-Sardinia Channel	188.58	4.53
13	48UR20090508/		**3.044**
	DT1-Tyrrhenian North	180.42	1.59
	DT3-Tyrrhenian South	181.78	2.83
	DI1-Sardinia Channel	187.67	4.75
14	48UR20100430/		**5.44**
	DS2-Balearic Sea	194.39	3.15
	DF1-Algero-Provençal	192.67	4.69
	DS3-Algerian Basin	193.28	3.55
	DT1-Tyrrhenian North	184.26	2.23
	DT3-Tyrrhenian South	183.86	2.02
	DI1-Sardinia Channel	186.52	5.23
15	48UR20100731/		**6.21**
	DS1-Alboran Sea	186.58	3.68
	DS3-Algerian Basin	189.94	3.34
	DT1-Tyrrhenian North	178.03	2.22
	DT3-Tyrrhenian South	178.14	3.27
	DI1-Sardinia Channel	186.60	5.18
16	48UR20101123/		**3.96**
	DT1-Tyrrhenian North	186.29	3.86

https://doi.org/10.5194/essd-2024-365
Preprint. Discussion started: 20 September 2024

	DT3-Tyrrhenian South	181.04	1.68
17	48UR20110421/		**2.47**
	DT1-Tyrrhenian North	180.0	1.86
	DT3-Tyrrhenian South	179.4	2.80
18	48UR20111109/		**5.62**
	DF1-Algero-Provençal	191.20	3.92
	DT1-Tyrrhenian North	182.00	2.22
	DT3-Tyrrhenian South	182.79	3.15
	DI1-Sardinia Channel	185.19	5.43
20	48UR20120111//		**5.29**
	DF1-Algero-Provençal	192.90	4.35
	DT1-Tyrrhenian North	184.69	3.06
	DT3-Tyrrhenian South	184.17	2.88
	DI1-Sardinia Channel	186.06	5.60
21	48UR20121108/		**5.73**
	DF3-Ligurian Sea	197.73	5.27
	DT1-Tyrrhenian North	190.86	3.05
	DT3-Tyrrhenian South	189.89	2.85
	DI1-Sardinia Channel	196.25	5.42
211	48UR20130604/		**6.086**
	DF1-Algero-Provençal	192.907	4.337
	DS3-Algerian Basin	191.516	4.118
	DT1-Tyrrhenian North	183.228	3.139
	DT3-Tyrrhenian South	182.148	3.147
	DI1-Sardinia Channel	186.594	5.264
	DI3-Sicily Channel	178.630	0.531
22	48UR20131015/		**6.03**
	DF1-Algero-Provençal	195.96	4.90
	DS3-Algerian Basin	196.54	4.24
	DT1-Tyrrhenian North	188.79	4.38
	DT3-Tyrrhenian South	187.66	3.92
	DI1-Sardinia Channel	190.87	6.03
222	48QL20151123/		**4.27**
	DT1-Tyrrhenian North	183.17	3.84
	DT3-Tyrrhenian South	181.97	3.17
	DI1-Sardinia Channel	185.91	5.48
23	48QL20150804/		**5.79**
	DF3-Ligurian Sea	190.75	4.91
	DS2-Balearic Sea	191.13	3.21
	DF1-Algero-Provençal	190.32	4.43
	DS3-Algerian Basin	191.41	3.85
	DT1-Tyrrhenian North	184.60	3.60
	DT3-Tyrrhenian South	180.45	3.24
24	48QL20171023/		**7.195**
	DF1-Algero-Provençal	200.42	6.49
	DT1-Tyrrhenian North	193.62	5.53
	DT3-Tyrrhenian South	190.62	4.26
	DI1-Sardinia Channel	201.79	6.59
25[a]	48DP20180918/ DI3-Sicily Channel	-	-
27[a]	48DP20221015/ DI3-Sicily Channel	-	-
28[a]	48DP20230324/ DI3-Sicily Channel	-	-

[a] Cruises not included in the second QC. In bold: the overall standard deviation by cruise; in normal font: regional standard deviation by cruise.

3.2 Secondary quality control: crossover analysis

The secondary quality control (2nd QC) method involves comparing the CNR cruises with reference cruises, as described in Section 2.2. The reference data are considered to be accurate, precise and stable, particularly in deep water; however, this assumption may not always be effective, especially for recent cruises. There is a notable lack of comprehensive studies addressing the general trends of dissolved oxygen levels in the Mediterranean Sea.

- *Consistency of the reference data:*

Each profile from the reference cruises (see Table 2) was interpolated using a piecewise cubic Hermite interpolating scheme to standard pressure values ranging from 0 to 3600 dbar. Subsequently, all profiles were

https://doi.org/10.5194/essd-2024-365
Preprint. Discussion started: 20 September 2024

averaged to produce a single profile for each cruise. Figure 7 illustrates the ratio (A/B) estimates between the tested cruise (A:6/06MT20011018) and the remaining five reference cruises (B). The results indicate a significant difference in measurements from the surface to 1000 dbar, which may be attributed to seasonal variations and atmospheric interactions.

Below 1000 dbar, variability is reduced, with the ratio approaching 1, indicating good agreement among the cruises, with the exception of cruise 28/11BG20220517 (Fig. 7(e)). This particular cruise exhibited Oxygen levels approximately ~ 4% lower than those of the other reference cruises, as shown in Fig.4(b).

Observations from this cruise, conducted in 2022, may indicate natural variability in oxygen levels, suggesting a potential decline in oxygen levels in the WMED, similar to trends observed in other oceanic regions (Grégoire et al., 2023). However, it is important to consider that this discrepancy could also stem from the precision of the Winkler titration values and their standardization with potassium iodate (KIO3). A 4% difference in oxygen concentration is substantial and raises questions about the validity of such variation at these depths.

At depths below 2500 dbar, differences among the reference cruises were noted, revealing similar patterns with slight variations, that warrant further investigations in subsequent studies. With the exception of cruise 11BG20220517, the deep oxygen measurements exhibited a high degree of alignment across the cruises, indicating a strong agreement within the depth range of 1000 and 2000 db, where the minimum for transient tracers is typically located. this layer is characterized by lower temporal variability; thus, any change occuring below 1000 db do not significantly impact the results of the 2nd QC.

In this analysis, we assess the extent to which adjustments should be recommended. Following the standards established by CARINA and GLODAP data products, no adjustments smaller than 1% for oxygen measurements were applied (Hoppema et al., 2009). Overall, five out of six reference cruises demonstrated an average ratio below 1000 dbar, within the 1% accuracy limit (ranging from 0.99 to 1.01).

However, the deep average ratio for reference cruise 28/11BG20220517 was recorded at 0.97, indicating that its oxygen levels were 3% lower. We therefore did not accept this cruise as valid reference data.

https://doi.org/10.5194/essd-2024-365
Preprint. Discussion started: 20 September 2024

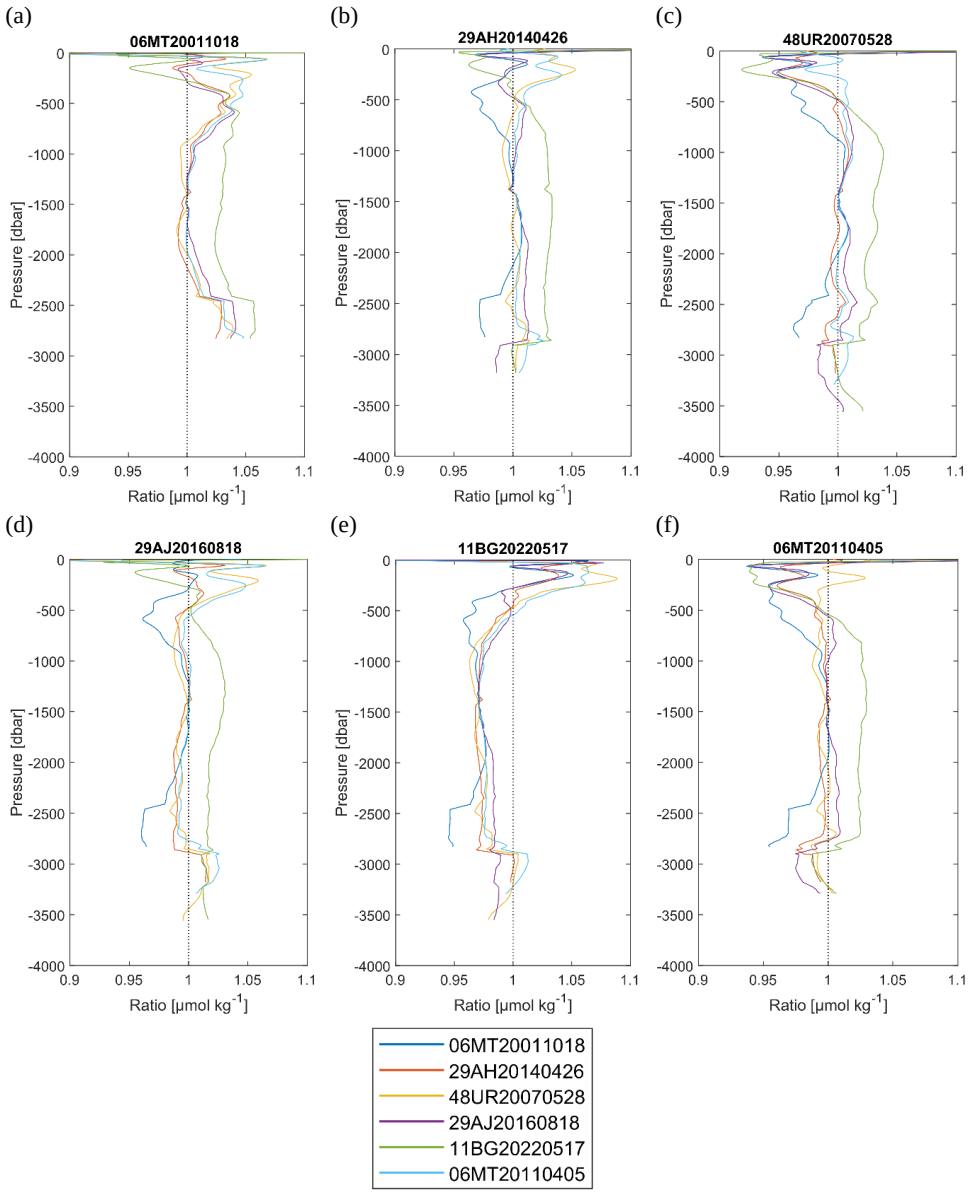

Figure 7. Vertical distribution of the ratio between the tested reference cruise (top of each subplot) vs the other references (in the legend box below).

https://doi.org/10.5194/essd-2024-365
Preprint. Discussion started: 20 September 2024

- *Crossover analysis:*

A crossover analysis, following the approach of Johnson et al. (2001) and Lauvset and Tanhua (2015), was conducted. This analysis is predicated on the comparison of cruise pairs, where the differences between two cruises within a predefined spatial distance, here a radius of 2° latitude (approximately 222 km) are assessed. In this process, the interpolated profiles for each station in cruise C1 were compared to the interpolated profiles from cruise C2 within the specified maximum distance. A difference profile was generated for each pair of stations, with a minimum of three stations required for each crossover. Calculations were performed on density surfaces to ensure that data comparisons were made between the same or comparable water masses, thereby mitigating biases associated with variations in salinity.

Density values were calculated for each measurement, and data from each profile were interpolated using a piecewise cubic Hermite interpolating scheme to standard density levels. This iterative process was repeated for each station in the cruise, resulting in multiple difference profiles. The outcome is the weighted mean and standard deviation of the difference profiles for each cruise, referred to as the offset. The weighting applied to the profiles is based on their variability, giving higher importance to parts of the profiles with lower variability (adapted from Tanhua et al. 2010, 2015). This approach accommodates potential variability in deep layers, particularly in the Mediterranean Sea, which is influenced by ventilation processes (Testor et al., 2018).

Figure 8 illustrates an example of a crossover and offset between cruise pairs, while an overview of some crossovers vs. reference dataset are displayed in Section 4. All calculated offsets for each cruise were examined to determine the presence of any likely biases in the measurements.

Corrections were meticulously reviewed and justified whenever adjustments were deemed necessary (Table 4). It is important to note that high variability in deep-water of the Mediterranean Sea, particularly in the Northern WMED where deep convection occurs, may increase the likelihood of detecting offsets in unbiased data.

The number of stations in the overlapping region (i.e., within the predefined radius) is critical for accurate offset estimation. For instance, as depicted in Figure 8 (a), 27 stations from C1 were compared to 15 stations from C2 to estimate the offset; a limited number of stations can introduce uncertainty into the offset estimate. Additionally, while the number of crossover cruises is significant, the Mediterranean Sea has a limited number of reference cruises available.

Following adjustments, the last step involves evaluation the overall internal consistency of the CNR-O2WMED using the weighted mean (WM) of the absolute offsets (D) of all crossovers (L) and the standard deviation (σ), following Tanhua et al. (2009) and Belgacem et al. (2020). This assessment quantifies the accuracy of the data product, as supported by previous studies (Hoppema et al., 2009; Sabine et al., 2010; Tanhua et al., 2009). Notably, our evaluation is based on offsets relative to a reference dataset, providing a comprehensive understanding of data consistency.

$$\mathrm{WM}=\frac{\sum_{i=1}^{L} D(i)/(\sigma(i))^2}{\sum_{i=1}^{L} 1/(\sigma(i))^2}$$

https://doi.org/10.5194/essd-2024-365
Preprint. Discussion started: 20 September 2024

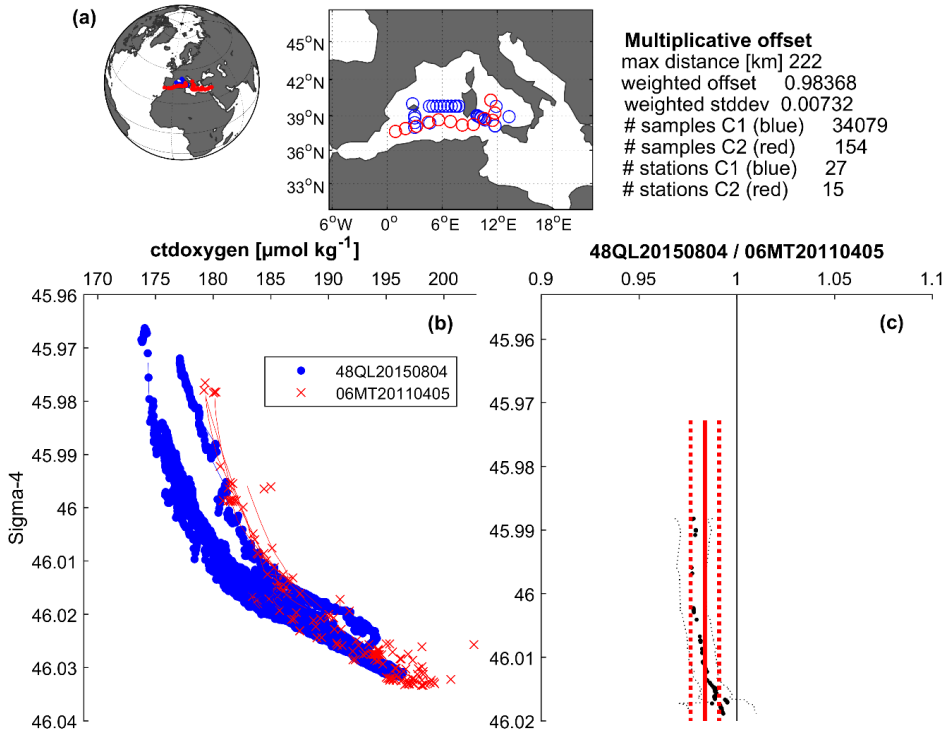

Figure 8. An illustration showcasing the calculated offset for dissolved oxygen between cruise 48QL20150804 and cruise 06MT20110405 (reference cruise). (a) Spatial distribution of CTD stations involved in the crossover analysis, along with statistical information. (b) Vertical profiles of dissolved oxygen observation (µmol kg^{-1}) from both cruises that fall within the radius of 2° (>1000 dbar). (c) Display of the difference between both cruises (thick dotted black line), standard deviation (thin dotted black lines), the weighted average of the offset (solid red line), and h the weighted standard deviation (dotted red line)

4 Results of the secondary QC and recommendations

The outcomes of the crossover analysis applied to the CNR dissolved oxygen CTD data collected in the WMED are presented in terms of correction factors derived from comparisons with selected reference cruises (GLODAP, CARIMED, MedSHIP). These corrections, aimed at enhancing measurement consistency, are summarized in Table 4. The analysis assumes that the reference dataset represents the true values. This section details the various crossovers, discusses the offsets, and outlines the derived correction factors.

Each crossover was thoroughly evaluated, and corrections were refined as necessary, considering the number of crossovers and the stations involved in each comparison. The offsets and correction factors for each cruise indicated that a significant number of cruises fell outside the predefined accuracy envelope of 1% (as discussed in Section 3.2) and therefore required adjustments. Notably, cruises no. 25, no. 27, and no. 28 were excluded from the crossover analysis due to an insufficient number of stations below 1000 dbar; however, these cruises remain available in the data product.

In total, 73 crossovers were identified. The analysis suggested that deep oxygen measurements from specific cruises (no. 2, no. 8, no. 9, no. 15, no. 17, no. 211, no. 222, and no.23) necessitated upward adjustment when

https://doi.org/10.5194/essd-2024-365
Preprint. Discussion started: 20 September 2024

compared to the reference cruises in the region. Conversely, cruises no. 3, no. 5, no. 21, and no. 24 exhibited slightly elevated values relative to the respective reference datasets, indicating a need for downward adjustments.

Eight cruises (no. 6, no. 10, no.11/12, no. 13, no. 14, no. 16, no. 18, no. 20, and no.22) did not require any corrections, demonstrating consistency with the reference dataset and indicating a high quality of the measurements. A correction is endorsed when the offset exceeds the predefined accuracy envelope of ±1%. Overall, minor adjustments are proposed, reflecting the overall good quality of the data.

The range of all correction factors was 0.097 (difference between minimum and maximum value), with the most substantial correction factor reaching 1.05, assigned to cruise 48UR20130604 (no. 211). Correction factors varied between 0.95 and 0.975 (for adjustments <1) and between 1.018 and 1.05 (for adjustments > 1; refer to Table 4 and Fig. 9).

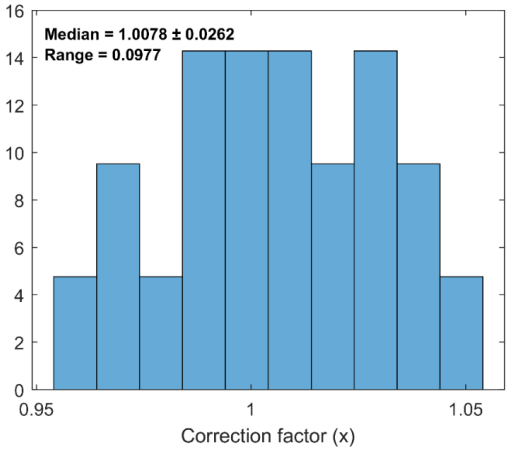

Figure 9. Distribution of multiplicative correction factor.

Table 5, Figure 10, and Figure S1 assesses the possible improvements after corrections. In the subsequent text, a thorough discussion about the adjustments (i.e., Correction factor) of the main challenging cruises is provided. The reader is invited to compare the descriptions with the respective plots in Figure 10 and the corresponding crossover summary figures for each cruise.

https://doi.org/10.5194/essd-2024-365
Preprint. Discussion started: 20 September 2024

Table 4. Summary of the suggested multiplicative adjustments for dissolved oxygen (x) resulting from the crossover analysis.

Cruise ID	EXPOCODE	Correction factor (*x*)
2	48UR20041006	1.039
3	48UR20050412	0.975
5	48UR20051116	0.955
6	48UR20060608	1
8	48UR20060928	1.031
9	48UR20071005	1.025
10	48UR20080318	1
11/12[a]	48UR20080905/48UR20081103	1
13	48UR20090508	1
14	48UR20100430	1
15	48UR20100731	1.034
16	48UR20101123	1
17	48UR20110421	1.022
18	48UR20111109	1
20	48UR20120111	1
21	48UR20121108	0.973
211	48UR20130604	1.052
22	48UR20131015	1
222	48QL20151123	1.039
23	48QL20150804	1.018
24	48QL20171023	0.970

[a] Cruise #11 and cruise #12 were merged in the secondary QC.

Cruise no. 2 (48UR20041006) has crossovers with four references. Notably, the crossover with the reference 06MT20011018 indicated that cruise no.2 had lower values, attributed to the limited number of crossover stations available for comparison. The remaining three reference cruises demonstrated a consensus regarding a mean offset of 0.96 (Fig. 10). The offset observed between cruise 48UR20041006 and the reference 06MT20110405 (7 years difference), 29AH20140426 (10 years difference) and 29AJ20160818 (12 years difference) suggest a 4% increase. While this increase may appear excessive, it is important to consider that the regional deep averages obtained from cruise no.2 (Table3) were the lowest. This may provide a rational for the adjustment.

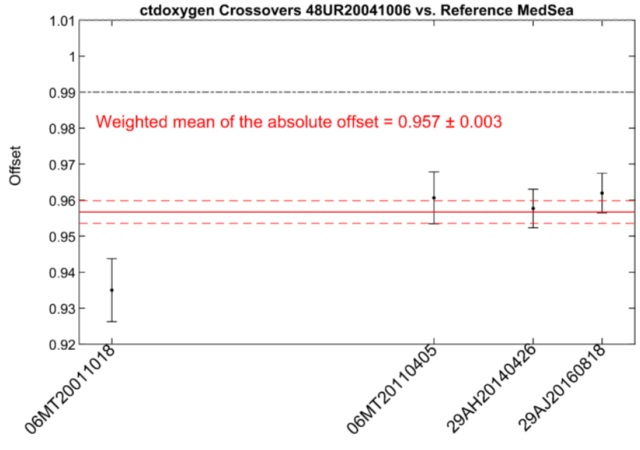

Figure 10. Summary of offsets for all crossovers found for CTD oxygen on cruise no. 2/48UR20041006. The solid red line indicates the weighted mean of the offsets, with its standard deviation in dashed lines; the dashed grey lines denote the predefined accuracy limits for Oxygen measurements; the black dots with

https://doi.org/10.5194/essd-2024-365
Preprint. Discussion started: 20 September 2024

error bars illustrate the weighted mean offsets in relation to individual reference cruises, along with their corresponding weighted standard deviations. The weighted mean and standard deviation of these offsets are annotated within the figure. Note that the reference cruises along the x-axis are arranged in chronological order.

Data from cruise **no.3 48UR20050412** was compared to the same reference cruises as cruise no.2. The offset between cruise no.3 and the reference cruises indicates that an adjustment to decrease oxygen is necessary. As pointed out in section 3.1 cruise no.3 exhibited low precision compared to cruises conducted in the same regions. Besides, Figures 10 and 11 illustrate similar behaviors with the reference dataset. For this cruise, the offset is 1.025 which supports a downward adjustment of ~3%.

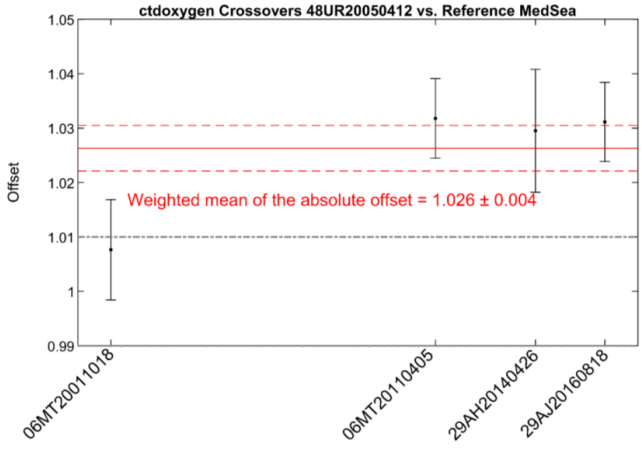

Figure 11. the same as Fig.10 but for no.3 48UR20050412

Cruise **no. 5 (48UR20051116)** had two crossovers with the references 06MT20110405 and 29AJ20160818 (Fig.12). An offset of 1.045 is computed. Based on this, an adjustment toward a decrease of ~5% is suggested for cruise no.5. The discrepancy may indicate potential issues with Winkler values or sensor calibration.

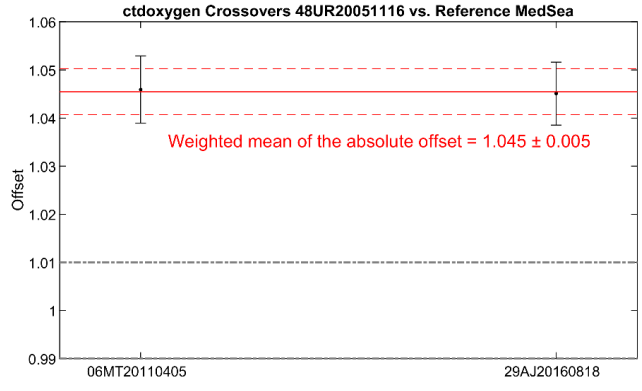

Figure 12. the same as Fig.10 but for no. 5 (48UR20051116)

https://doi.org/10.5194/essd-2024-365
Preprint. Discussion started: 20 September 2024

Cruise no. 6 (48UR20060608) has five crossovers (Fig. 13). This cruise has few crossover stations with cruise 48UR20070528 which appears to explain the quite large 1.06 offset. The decrease in the measurements is perceived with crossovers 29AH20140426 and 29AJ20160818 which pointed to similar offset of 1.026 which means a downward correction of 3%.

While crossovers with 06MT20110405 and 06MT20011018 do not propose any offset, and cruise no.6 seemed to agree in some parts of the crossing regions;

We refrained from adjusting the data because most of the crossovers did not show consistency and there was good agreement with the references of years 2001 and 2011.

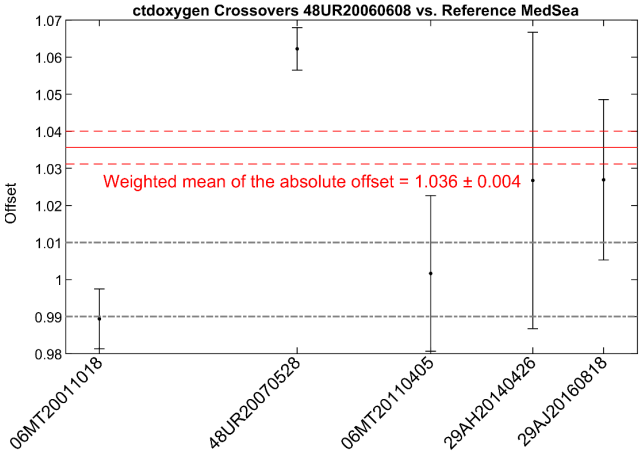

Figure 13. the same as Fig.10 but for Cruise no. 6 (48UR20060608)

Cruise no. 8 (48UR20060928) has three crossovers in the Tyrrhenian Sea with reference cruises 06MT20110405, 29AH20140426 and 29AJ20160818 (Fig. 14). All three offsets (0.97) point to the same correction toward an increase of 3%. An adjustment of 1.03 is recommended.

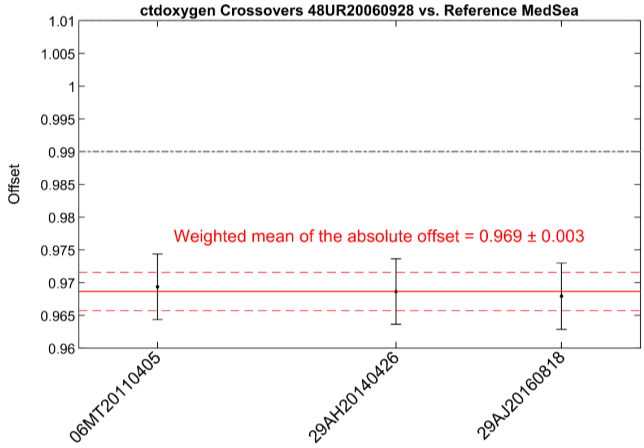

https://doi.org/10.5194/essd-2024-365
Preprint. Discussion started: 20 September 2024

Figure 14. the same as Fig.10 but for Cruise no. 8 (48UR20060928).

Cruise no. 9 (48UR20071005) has four crossovers. All showing an offset of 0.97 except the crossover with 06MT20011018, where the offset is about 0.95 (Fig. 15). This seems to be large because of the large scatter of the few stations in the crossing region. Considering the crossovers with 06MT20110405 29AH20140426 and 29AJ20160818, an adjustment of 3% toward an increase is recommended.

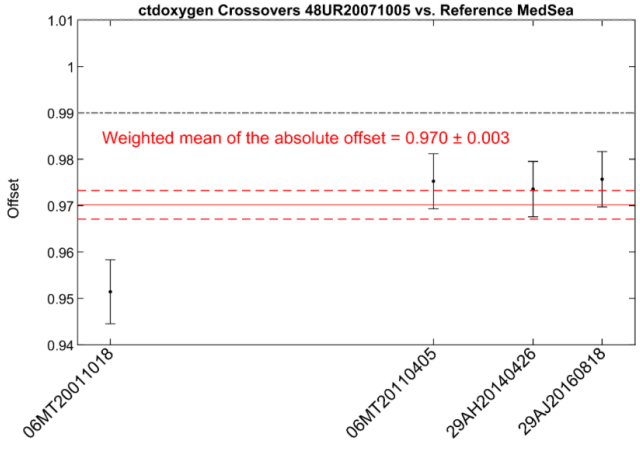

Figure 15. the same as Fig.10 but for Cruise no. 9 (48UR20071005)

Cruise no. 11 (48UR20080905) has no crossover points with the selected reference dataset. Since it has a two-month difference from the same year of **cruise no. 12 (48UR20081103)**, both cruises were merged. This 2008 cruise has five crossovers. Crossovers with 06MT20011018 show a large offset of 0.97 which means an increase of 3%. Though, crossover with 48UR20070528 shows a large offset of 1.03 suggesting a decrease of 3%. Both crossovers have three crossover points disseminated in different subregions. Their offsets are noticeably higher when compared to the offsets observed in crossovers with the reference cruises 06MT20110405, 29AH20140426 and 29AJ20160818 (Fig.16). However, cruise no.11/12 conducted in 2008, consistently shows no significant offset. Based on this evidence and the inconsistency in the 2001 and 2007 crossovers, we decided for no adjustments

https://doi.org/10.5194/essd-2024-365
Preprint. Discussion started: 20 September 2024

Open Access Earth System Science Data Discussions

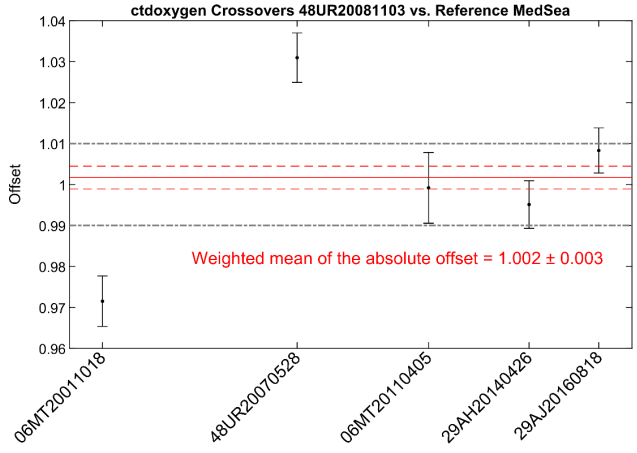

Figure 16. the same as Fig.10 but for Cruise no. 11 and no. 12.

Cruise no. 15 (48UR20100731) has four crossovers. Crossover with 06MT20011018 show very large offset of 0.95 suggesting 5% increase. With few stations in the crossing regions, this crossover is not warrant of reliable adjustment.

Crossovers with 06MT20110405 (one year difference), complies with the singular crossovers with the reference 29AH20140426 (4 years difference) and 29AJ20160818 (six years difference) about an offset of ~0.97 (Fig.17), which gives further evidence for an adjustment of 3% increase.

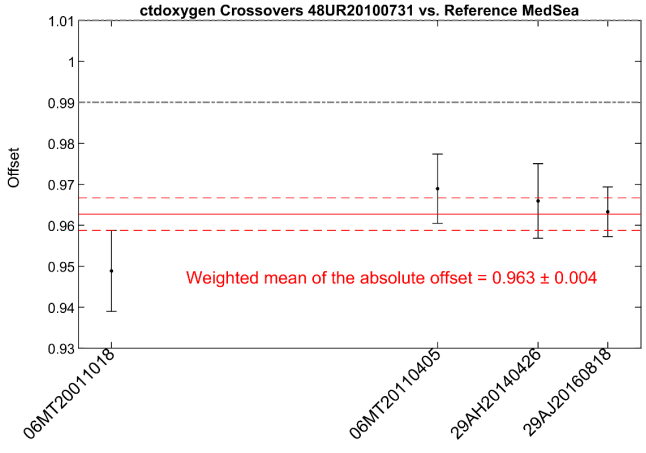

Figure 17. The same as Fig.10 but for Cruise no. 15 (48UR20100731).

Cruise no. 17 (48UR20110421) has two crossovers in the Tyrrhenian Sea both agree about an offset of 0.97 (Fig.18). Based on this, an adjustment of 2% toward an increase is suggested. Crossover with same year reference cruise 06MT20110405 gave offset of 0.97. Same offset and adjustments are suggested to cruise no. 8

https://doi.org/10.5194/essd-2024-365
Preprint. Discussion started: 20 September 2024

(48UR20060928) in the same region. This demonstrates additional evidence about the suggested adjustment of cruise no.17, to make it consistent with the neighboring cruises.

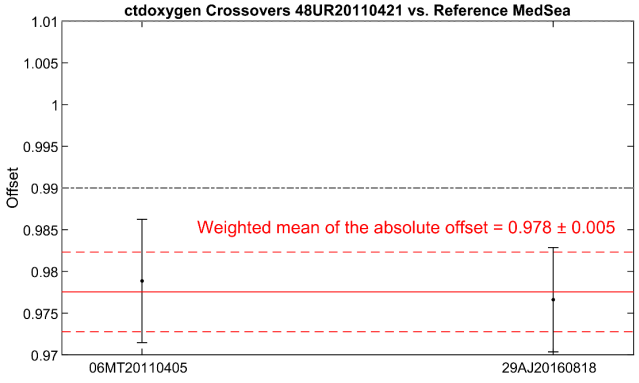

Figure 18. The same as Fig.10 but for Cruise no. 17 (48UR20110421)

Cruise no. 18 (48UR20111109) has four crossovers. Offsets with the same year reference cruises 06MT20110405 are in good agreement, same with offsets computed with 29AH20140426 (3 years difference) and 29AJ20160818 (5 years difference) that were 0.99 (Fig. 19). Except with crossover with 06MT20011018 (10 years difference) suggestion an offset of 0.97 and an adjustment of 2% increase. Few crossover stations are used to estimate the offset which explains the large offset compared to the other reference. Hence, we have concluded to refrain from making any adjustments.

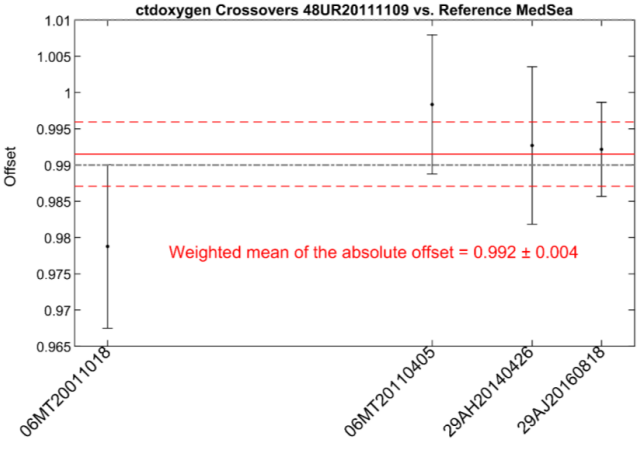

Figure 19. the same as Fig.10 but for Cruise no. 18 (48UR20111109).

Cruise no. 21 (48UR20121108) has three crossovers with the reference cruises (Fig. 20). In view of crossovers with 06MT20110405 (one year difference), an offset of 1.026 is found suggesting that the data appear high than the reference and require a downward adjustment of ~3%. The adjustment appears justified because the offset

https://doi.org/10.5194/essd-2024-365
Preprint. Discussion started: 20 September 2024

435 with the references 29AH20140426 and 29AJ20160818 suggest similar offset magnitude. Consequently, the
436 adjustment was set to a decrease of 3%.

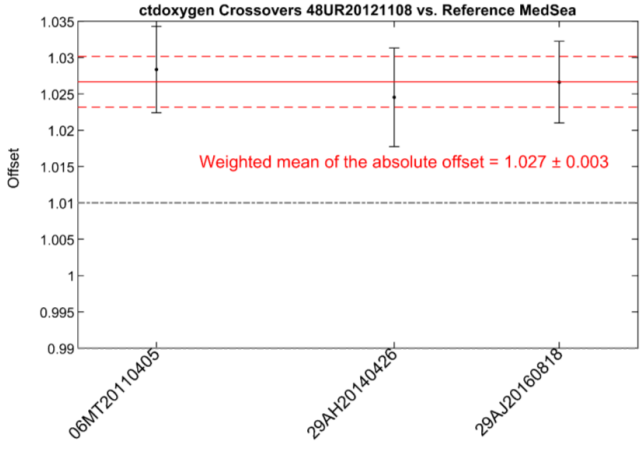

437

438 **Figure 20. The same as Fig.10 but for Cruise no. 21 (48UR20121108).**

439 **Cruise no. 211 (48UR20130604)** has an offset of 5% of similar magnitude in all crossovers with the four reference
440 cruises 06MT20011018, 06MT20110405, 29AH20140426 and 29AJ20160818 (Fig. 21). Cruise **48UR20130604**
441 seems to be high. Connecting it to cruise **no. 22 (48UR20131015)** from the same year, this cruise is in good accord
442 with the same reference cruises in the same crossing areas and did not show any offset, providing additional
443 evidence. We think that an adjustment of 5% toward an increase is justified to bring the data within the acceptable
444 range.

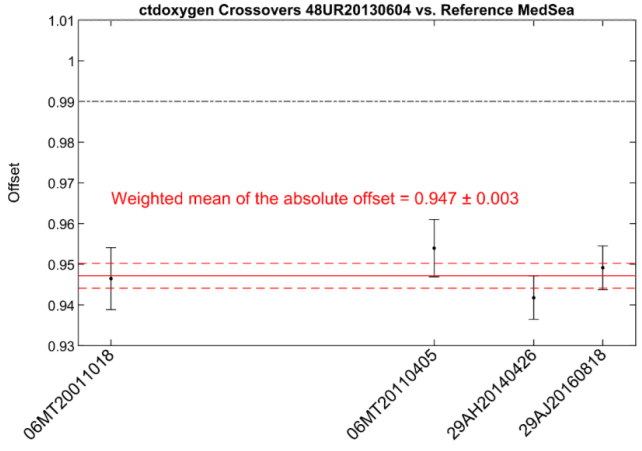

445

446 **Figure 21. The same as Fig.10 but for Cruise no. 211 (48UR20130604).**

447 **Cruise no. 222 (48QL20151123)** has a consistent offset of 0.96 with all three crossovers spanning different years
448 with cruises 06MT20110405 (four-year difference), 29AH20140426 (one year difference) and 29AJ20160818 (1

https://doi.org/10.5194/essd-2024-365
Preprint. Discussion started: 20 September 2024

year difference) (Fig. 22). Deep measurement from this cruise seems to be lower than the reference suggesting a correction of 4% toward an increase.

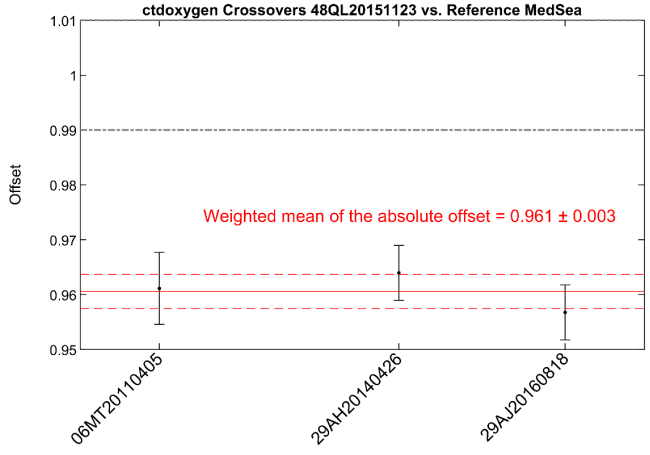

Figure 22. The same as Fig.10 but for Cruise no. 222 (48QL20151123).

Similar increase is apparent in **Cruise no. 23 (48QL20150804)** happened in the same year 2015. Three crossovers with the references 06MT20110405, 29AH20140426 and 29AJ20160818 agree about a ~2% increase based on a mean offset of 0.98 (Fig. 23), whereas crossover with the reference cruise 06MT20011018 (14 years difference) propose an offset of 0.96, accordingly 4% increase, which is very high and not enough justified. We therefore suggest a correction following the three references.

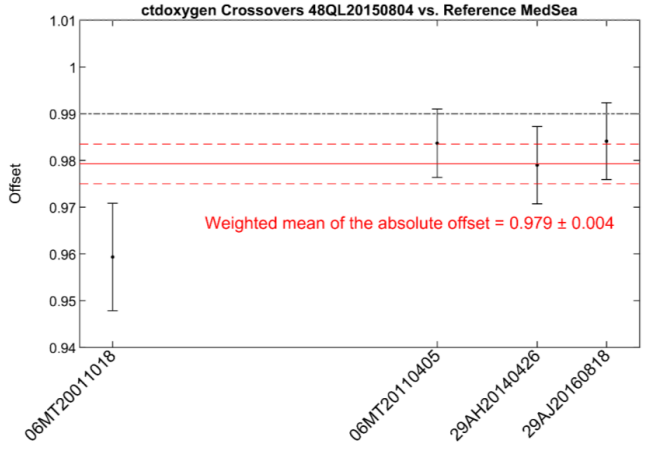

Figure 23. The same as Fig.10 but for Cruise no. 23 (48QL20150804).

And finally, **cruise no. 24 (48QL20171023)** has three crossovers (Fig. 24) with the reference 06MT20110405 (six years difference), 29AH20140426 (three years) and 29AJ20160818 (one year difference). A constant offset of 1.029 is assessed indicating that cruise no.24 is higher than the reference. The offset appears to be persistent in all

https://doi.org/10.5194/essd-2024-365
Preprint. Discussion started: 20 September 2024

these years and is suggestive of an adjustment of 3% toward a decrease, that should be appropriate. We decided to follow the suggestion.

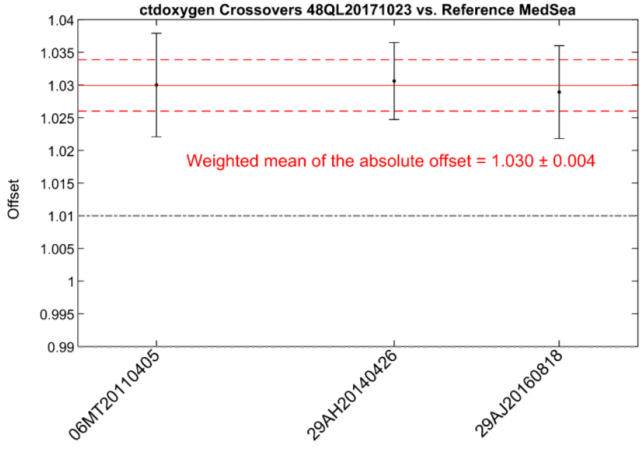

Figure 24. The same as Fig.10 but for Cruise no. 24 (48QL20171023).

To validate our findings, we recalculated the offsets using the adjusted data after applying the corrections outlined in Table 4.

Following the application of these adjustments, the offsets were reduced. The suggested cruises now fall within the accepted envelope of 1% indicating an enhanced consistency of the measurements. This improvement is evident in the adjusted data presented in Figure 25 (in blue) and table 4.

To evaluate the consistency, we computed WM of the absolute offsets. The consistency of the adjusted oxygen dataset experienced a slight enhancement, increasing from 0.991 to 0. 998%. This corresponds to an improvement in the internal consistency of the dataset by 0.7%. The minor improvement in consistency, coupled with the reduced range, underscores the high quality of the initial dataset and efficacy of the quality assurance procedures implemented during each cruise.

The adjustments removed potential biases arising from errors related to measurement, calibration, data handling practices, and the lack of adherence to international standards improving the overall consistency.

https://doi.org/10.5194/essd-2024-365
Preprint. Discussion started: 20 September 2024

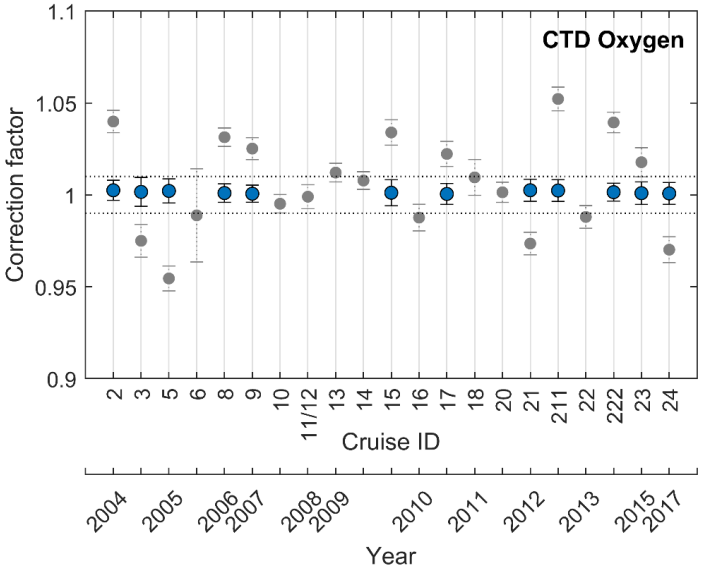

Figure 25. Results of the crossover analysis results for CTD dissolved oxygen, showing the correction before (in grey) and after (in blue) adjustment. Error bars indicate the standard deviation of the absolute weighted offset. A correction means the original CTD Oxygen data must be multiplied by that amount (see Table 4). The dashed line represents the 1% accuracy envelope for an adjustment to be made.

Table 5. Results from the Secondary QC: improvements of the weighted mean of absolute offset per cruise for both unadjusted and adjusted data. "n" represents the number of crossovers per cruise. Values in bold (>1) signify instances where the measurements from the tested cruises are lower than the reference data.

Cruise ID	EXPOCODE	CTD Oxygen (%)			Crossover regions
		n	Unadjusted	Adjusted	
2	48UR20041006	4	**0.96** ±0.006	0.99±0.005	Tyrrhenian sea Algerian basin Alboran sea
3	48UR20050412	4	1.025±0.008	0.99±0.007	Tyrrhenian sea Sicily-Sardinia Channel Algerian basin Alboran sea
5	48UR20051116	2	1.045±0.006	0.99±0.006	Tyrrhenaian Sea Sicily-Sardinia Channel
6	48UR20060608	5	1.01±0.02	NA	Ligurian Sea Tyrrhenain Sea Algerian basin Saridinia-Balearic sea
8	48UR20060928	3	**0.96**±0.005	0.99±0.005	Ligurian Sea Tyrrhenain Sea Algerian basin Saridinia-Balearic sea
9	48UR20071005	4	**0.97**±0.005	0.99±0.004	Tyrrhenain Sea Algerian basin Saridinia-Balearic sea
10	48UR20080318	2	1.004±0.005	NA	Tyrrhenain Sea
11/ 12	48UR20080905/ 48UR20081103	5	1.001±0.006	NA	Tyrrhenaian Sea Sicily-Sardinia Channel Algerian Basin Alboran Sea
13	48UR20090508	**3**	**0.989**±0.005	NA	Tyrrhenian Sea

https://doi.org/10.5194/essd-2024-365
Preprint. Discussion started: 20 September 2024

					Sicily-Sardinia channel
14	48UR20100430	**4**	**0.99**±0.004	NA	Tyrrhenain Sea Algerian basin Saridinia-Balearic sea Sicily-Sardinia channel
15	48UR20100731	4	**0.96**±0.006	0.999±0.007	Tyrrhenian Sea Sicily-Sardinia channel Algerian basin Alboran Sea
16	48UR20101123	2	1.012±0.07	NA	Tyrrhenian Sea
17	48UR20110421	2	**0.97±0.006**	0.999±0.005	Tyrrhenian Sea Sicily-Sardinia channel
18	48UR20111109	4	**0.99±0.009**	NA	Tyrrhenain Sea Algerian basin Saridinia-Balearic sea
20	48UR20120111	4	**0.99±±0.005**	NA	Tyrrhenain Sea Sicily-Sardinia channel Algerian basin Saridinia-Balearic sea
21	48UR20121108	3	1.026±±0.006	0.99±0.006	Tyrrhenain Sea Saridinia-Balearic sea Sardinia channel
211	48UR20130604	4	**0.950±±0.006**	0.997±0.005	Tyrrhenain Sea Sicily-Sardinia channel Algerian basin Saridinia-Balearic sea
22	48UR20131015	4	1.012±0.006	NA	Tyrrhenain Sea Sicily-Sardinia channel Algerian basin Saridinia-Balearic sea
222	48QL20151123	3	**0.96**±0.005	0.998±0.004	Tyrrhanaian Sea Sicily-Sardinia channel
23	48QL20150804	4	**0.98**±0.007	0.999±0.006	Ligurian Sea Tyrrhenain Sea Algerian basin Saridinia-Balearic sea
24	48QL20171023	3	1.029±±0.007	0.99±0.005	Tyrrhanaian Sea Sicily-Sardinia channel

5 Summary and conclusions

This study's main objective was to enhance data quality, assurance, and accessibility within the context of FAIR data principles. Acknowledging the limitations of the reference datasets is essential; although considered high quality, they are not infallible and may not fully cover the entire temporal range of interest. Regardless, our quality control efforts have yielded positive results, as demonstrated throughout this study.

The majority of the CTD oxygen data now falls within the predefined acceptance range of 1%, indicating a consistent and accurate dataset. This aligns with established standards seen in widely used datasets, such as CARINA and GLODAP (Hoppema et al., 2009, Tanhua et al., 2009). Furthermore, the adjustments made to address systematic biases between reference datasets and the CNR cruises have significantly improved the internal consistency of Oxygen measurements.

Despite the inherent challenges in assessing changes in oxygen levels due to the scarcity of measurements, the recent oxygen data contribute substantially to our understanding of oxygen variability in the region.

The CNR-O2WMED dataset serves as a valuable regional resource, providing quality-controlled measurements that facilitate accurate trend quantification and estimation of changes, thereby making it an essential tool for future

https://doi.org/10.5194/essd-2024-365
Preprint. Discussion started: 20 September 2024

studies with acceptable temporal and spatial coverage, and the potential extension of the analysis to the Eastern Mediterranean Sea. The utility of this dataset extends to its assimilation into ocean models and the verification of regional models, offering critical insights in the oxygen cycle.

As we face warming ocean and increased stratification, the anticipated decline in oxygen levels may lead to enhanced acidification and reduced CaO_3, potentially accelerating in the remineralization of organic matters at shallower depths. Consequently, the expansion of low oxygen zones is expected, posing significant ecological challenges (Keeling and al., 2009).

While the current dataset does not incorporate data from various sources to avoid potential inconsistencies, ensuring the reliability of the CNR-O2WMED data remains a priority before any future integrations. The dataset's utility will be maximized when used in conjunction with other data sources, such as BGC-Argo and glider data, allowing for more comprehensive analysis of the oxygen dynamics in the WMED.

Future studies should focus on synergizing regional datasets to enhance our understanding of ongoing changes in Biogeochemical cycles. This collaborative approach will ultimately contribute to global efforts to monitor and mitigate the impacts of ocean deoxygenation, fostering a deeper understanding of biogeochemical processes and their implications for marine ecosystems.

Future studies should focus on synergizing regional datasets to enhance our understanding of the ongoing changes, ultimately contribution to global efforts to monitor and mitigate the impact of ocean deoxygenation.

6 Data availability

The CNR_O2WMEDv1 (Belgacem et al., 2024 [in review], see temporary link below) dataset is available at PANGAEA (submitted on 21/08/2024, DOI in preparation). It consists of two parts; the first is the original data product which has undergone both calibration and 1st quality check. The second is the original product adjusted using the recommended corrections from the secondary quality control. The dataset is complementary to the data product CNR-DIN-WMED available https://doi.org/10.1594/PANGAEA.904172. No special software is required to access the data.

Temporary link to CNR_O2WMED_ODV format:

https://cnrsc-my.sharepoint.com/:f:/g/personal/malekbelgacem_cnr_it/EkIgo958UMlBmJ8SGwNB4HwBBX-FzDa8Nl9C3vHeS4Vd4Q?e=Wt8p1I

Table 6 summarizes the list of parameters included.

Table 6. Summary of data product parameters and units.

Variable	Data Product file parameter name	Data product WOCE flag name	Units
Expedition/cruise code	EXPOCODE		
Cruise ID	CRUISE		
Station number	STNNBR		
Year	YEAR		
Month	MONTH		
Day	DAY		
Latitude	LATITUDE		decimal degree

https://doi.org/10.5194/essd-2024-365
Preprint. Discussion started: 20 September 2024

Longitude	LONGITUDE		decimal degree
Pressure	CTDPRS		decibar
Temperature	CTDTMP		°C
Salinity	CTDSAL	CTDSAL_FLAG_W	
Oxygen	CTDOXY	CTDOXY_FLAG_W	µmol kg^{-1}

532

533

534 **Authors contributions**

535 MaB ran the analysis and wrote the manuscript. KS contributed to writing the manuscript. MA, SKL contributed
536 to the analysis. JC contributed to specific parts of the manuscript. MiB and SS coordinated the technical aspects
537 of most of the cruises. CC and TC assisted some of the chemical analysis and contributed to write the analytical
538 method.

539 **Competing interest**

540 The authors declare that they have no conflict of interest.

541 **Acknowledgements**

542 The data have been collected in the framework of several national and European projects, e.g. KM3NeT, EU GA
543 no. 011937; SESAME, EU GA no. GOCE-036949; PERSEUS, EU GA no. 287600; OCEAN-CERTAIN, EU GA
544 no. 603773; COMMON SENSE, EU GA no. 228344; EUROFLEETS, EU GA no. 228344; EUROFLEETS2, EU
545 GA no. 312762; JERICO, EU GA no. 262584; and the Italian PRIN 2007 program "Tyrrhenian Seamounts
546 ecosystems" and the Italian RITMARE flagship project, both funded by the Italian Ministry of Education,
547 University and Research. The authors thank the Horizon Europe – IA REDRESS project for the funding.

548 The authors are deeply indebted to all investigators and analysts who contributed to data collection at sea during
549 so many years as well as to the PIs of the cruises (Stefano Cozzi, Gabriella Cerrati, Stefano Aliani, Mario Astraldi,
550 Maurizo Azzaro, Alberto Ribotti, Massimiliano Dibitetto, Gian Pietro Gasparini, Annalisa Griffa, Jeff Haun, Loïc
551 Jullion, Gina La Spada, Elena Mannini, Angelo Perilli and Chiara Santinelli), the captains, and the crews for
552 allowing the collection of this enormous dataset; without them, this work would not have been possible.

553 **Reference**

554 Belgacem, M., Chiggiato, J., Borghini, M., Pavoni, B., Cerrati, G., Acri, F; Cozzi, S., Ribotti, A., Álvarez, M.,
555 Lauvset, S. K., and Schroeder, K.: Quality controlled dataset of dissolved inorganic nutrients in the western
556 Mediterranean Sea (2004– 2017) from R/V oceanographic cruises, PANGAEA [data set],
557 https://doi.org/10.1594/PANGAEA.904172, 2019.
558 Belgacem, M., Chiggiato, J., Borghini, M., Pavoni, B., Cerrati, G., Acri, F., Cozzi, S., Ribotti, A., Álvarez, M.,
559 Lauvset, S. K., and Schroeder, K.: Dissolved inorganic nutrients in the western Mediterranean Sea (2004–2017),
560 Earth Syst. Sci. Data, 12, 1985–2011, https://doi.org/10.5194/essd-12-1985-2020 , 2020.
561 Belgacem, M., Schroeder, K., Lauvset, SK., Álvarez, M., Chiggiato, J., Borghini, M., Cantoni, C., Ciuffardi, T.,
562 Sparnocchia, S.: O2WMED: Quality controlled dataset of dissolved oxygen in the western Mediterranean Sea
563 (2004-2023) from R/V oceanographic cruises [dataset], PANGAEA, in review: temporary link: https://cnrsc-

564 my.sharepoint.com/:f:/g/personal/malekbelgacem_cnr_it/EkIgo958UMlBmJ8SGwNB4HwBBX-
565 FzDa8Nl9C3vHeS4Vd4Q?e=Wt8p1I , 2024.

566 Coppola, L., Legendre, L., Lefevre, D., Prieur, L., Taillandier, V., & Riquier, E. D. (2018). Seasonal and inter-
567 annual variations of dissolved oxygen in the northwestern Mediterranean Sea (DYFAMED site). Progress in
568 Oceanography, 162, 187-201, https://doi.org/10.1016/j.pocean.2018.03.001, 2018.
569 Fichaut, M., Garcia, M. J., Giorgetti, A., Iona, A., Kuznetsov, A., Rixen, M., and Medar Group:
570 MEDAR/MEDATLAS 2002: A Mediterranean and Black Sea database for operational oceanography, Elsevier
571 Oceanography Series, 69, 645–648, https://doi.org/10.1016/S0422-9894(03)80107-1 , 2003.
572 Grasshoff, K., Ehrhardt, M., and Kremling, K.: Methods of Seawater Analysis, 2nd Edition, Verlag Chemie
573 Weinhein, New York, 419 p., 1983.
574 Grasshoff, K., Kremling, K., and Ehrhardt, M.: Methods of seawater analysis (3rd edn.), Weinheim Press, WILEY-
575 VCH, 203–273, 1999.
576 Grégoire, M., Oschlies, A., Canfield, D., Castro, C., Ciglenečki, I., Croot, P., Salin, K., Schneider, B., Serret, P.,
577 Slomp, C.P., Tesi, T., Yücel, M. (2023). Ocean Oxygen: the role of the Ocean in the oxygen we breathe and the
578 threat of deoxygenation. Rodriguez Perez, A., Kellett, P., Alexander, B., Muñiz Piniella, Á., Van Elslander, J.,
579 Heymans, J. J., [Eds.] Future Science Brief No . 10 of the European Marine Board, Ostend, Belgium. ISSN: 2593-
580 5232. ISBN: 9789464206180. DOI: 10.5281/ zenodo.7941157, 2023.
581 Guy, S.-V., Kress, N., Silverman, J., Gertner, Y., Ozer, T., Biton, E., Lazar, A., Gertman, I., Rahav, E., and Herut,
582 B.: Post-eastern Mediterranean Transient Oxygen Decline in the Deep Waters of the Southeast Mediterranean Sea
583 Supports Weakening of Ventilation Rates, Front. Mar. Sci., 7, https://doi.org/10.3389/FMARS.2020.598686 ,
584 2021.
585 Hainbucher, D., Rubino, A., Cardin, V., Tanhua, T., Schroeder, K., and Bensi, M.: Hydrographic situation during
586 cruise M84/3 and P414 (spring 2011) in the Mediterranean Sea, Ocean Sci., 10, 669-682,
587 https://doi.org/10.5194/os-10-669-2014 , 2014.
588 Helen, R., Powley., Krom, M. D., Van Cappellen, P.: Circulation and oxygen cycling in the Mediterranean Sea:
589 Sensitivity to future climate change, J. Geophys. Res., https://doi.org/10.1002/2016JC012224 , 2016.
590 Hoppema, M., Velo, A., van Heuven, S., Tanhua, T., Key, R. M., Lin, X., Bakker, D. C. E., Perez, F. F., Ríos, A.
591 F., Lo Monaco, C., Sabine, C. L., Álvarez, M., and Bellerby, R. G. J.: Consistency of cruise data of the CARINA
592 database in the Atlantic sector of the Southern Ocean, Earth Syst. Sci. Data, 1, 63–75, https://doi.org/10.5194/essd-
593 1-63-2009 , 2009.
594 Janzen, C., Murphy, D., and Larson, N.: Getting more mileage out of dissolved oxygen sensors in long-term
595 moored applications, OCEANS 2007, IEEE, doi: 10.1109/OCEANS.2007.4449398, 2007.
596 Johnson, G. C., Robbins, P. E., and Hufford, G. E.: Systematic adjustments of hydrographic sections for internal
597 consistency, J. Atmos. Ocean. Tech., 18, 1234–1244, https://doi.org/10.1175/1520-
598 0426(2001)018<1234:SAOHSF>2.0.CO ;2, 2001.
599 Jullion, L.: TAlPro2016: A Tyrrhenian Sea & Alger-Provençal component of the MedSHIP Programme, RV
600 Angeles Alvariño, 18/08/16 – 29/08/16, Palermo (Italy) – Barcelona (Spain), Bremerhaven, EUROFLEETS2
601 Cruise Summary Report, https://epic.awi.de/id/eprint/49725/ , 2016.
602 Keeling, R. F., Körtzinger, A., and Gruber, N.: Ocean deoxygenation in a warming world, Annu. Rev. Mar. Sci.,
603 2, 199-229, doi: 10.1146/annurev.marine.010908.163855, 2010.

https://doi.org/10.5194/essd-2024-365
Preprint. Discussion started: 20 September 2024

Langdon, C.: Determination of Dissolved Oxygen in Seawater by Winkler Titration using Amperometric Technique, In: Hood, E.M., Sabine, C.L., Sloyan, B.M. (Eds.), The GO-SHIP Repeat Hydrography Manual: A Collection of Expert Reports and Guidelines, Version 1, IOCCP Report Number 14, ICPO Publication Series Number 134, 18pp., https://doi.org/10.25607/OBP-1350 , 2010.

Lauvset, S. K., and Tanhua, T.: A toolbox for secondary quality control on ocean chemistry and hydrographic data, Limnol. Oceanogr. Methods, 13, 601–608, https://doi.org/10.1002/lom3.10050 , 2015.

Laurent, C., Louis, L., Dominique, L., Louis, M. P., Vincent, T., Emilie, D., and Riquier, D.: Seasonal and inter-annual variations of dissolved oxygen in the northwestern Mediterranean Sea (DYFAMED site), Prog. Oceanogr., 162, 187-201, https://doi.org/10.1016/j.pocean.2018.03.001 , 2018.

Manca, B., Burca, M., Giorgetti, A., Coatanoan, C., Garcia, M. J., and Iona, A. Physical and biochemical averaged vertical profiles in the Mediterranean regions: an important tool to trace the climatology of water masses and to validate incoming data from operational oceanography, J. Mar. Syst., 48, 83–116, https://doi.org/10.1016/j.jmarsys.2003.11.025, 2004.

Álvarez, M., Catalá, T. S., Civitarese, G., Coppola, L., Hassoun, A. E. R., Ibello, V., Lazzari, P., Lefevre, D., Marcias, D., Santinelli, C., and Ulses, C: Chapter 11–Mediterranean Sea general biogeochemistry, Editor (s): Katrin Schroeder, Jacopo Chiggiato, Oceanography of the Mediterranean Sea, https://doi.org/10.1016/B978-0-12-823692-5.00004-2, 2022.

Martínez, J., Leonelli, F. E., García-Ladona, E., Garrabou, J., Kersting, D. K., Bensoussan, N., and Pisano, A.: Evolution of marine heatwaves in warming seas: the Mediterranean Sea case study, Front. Mar. Sci., 10, 1193164, https://doi.org/10.3389/fmars.2023.1193164, 2023.

Marullo, S., De Toma, V., di Sarra, A., Iacono, R., Landolfi, A., Leonelli, F., Napolitano, E., Meloni, D., Organelli, E., Pisano, A., Santoleri, R., and Sferlazzo, D.: Has the frequency of Mediterranean Marine Heatwaves really increased in the last decades? , EGU General Assembly 2023, Vienna, Austria, 23–28 Apr 2023, EGU23-4429, https://doi.org/10.5194/egusphere-egu23-4429 , 2023.

Mavropoulou, A.-M., Vervatis, V., and Sofianos, S.: Dissolved oxygen variability in the Mediterranean Sea, J. Mar. Syst., 208, 103348, https://doi.org/10.1016/j.jmarsys.2020.103348 ,2020.

Mavropoulou, A.-M.: Mediterranean Sea: Dissolved Oxygen, Temperature and Salinity Annual Variability and Monthly Climatology for the period 1960-2011, https://doi.org/10.5281/zenodo.3878076 , 2020.

Olsen, A., Key, R. M., van Heuven, S., Lauvset, S. K., Velo, A., Lin, X., Schirnick, C., Kozyr, A., Tanhua, T., Hoppema, M., Jutterström, S., Steinfeldt, R., Jeansson, E., Ishii, M., Pérez, F. F., and Suzuki, T.: The Global Ocean Data Analysis Project version 2 (GLODAPv2) – an internally consistent data product for the world ocean, Earth Syst. Sci. Data, 8, 297–323, https://doi.org/10.5194/essd-8-297-2016 , 2016.

Olsen, A., Lange, N., Key, R. M., Tanhua, T., Bittig, H. C., Kozyr, A., Álvarez, M., Azetsu-Scott, K., Becker, S., Brown, P. J., Carter, B. R., Cotrim da Cunha, L., Feely, R. A., van Heuven, S., Hoppema, M., Ishii, M., Jeansson, E., Jutterström, S., Landa, C. S., Lauvset, S. K., Michaelis, P., Murata, A., Pérez, F. F., Pfeil, B., Schirnick, C., Steinfeldt, R., Suzuki, T., Tilbrook, B., Velo, A., Wanninkhof, R., and Woosley, R. J.: An updated version of the global interior ocean biogeochemical data product, GLODAPv2.2020, Earth Syst. Sci. Data, 12, 3653–3678, https://doi.org/10.5194/essd-12-3653-2020 , 2020.

https://doi.org/10.5194/essd-2024-365
Preprint. Discussion started: 20 September 2024

642 Pastor, F., and Khodayar, S.: Marine heat waves: Characterizing a major climate impact in the Mediterranean,
643 EGU General Assembly 2023, Vienna, Austria, 24–28 Apr 2023, EGU23-13058,
644 https://doi.org/10.5194/egusphere-egu23-13058, 2023.
645 REALE, M., COSSARINI, G., LAZZARI, P., Lovato, T., Bolzon, G., Masina, S., Solidoro, C., and Salon, S.:
646 Acidification, deoxygenation, and nutrient and biomass declines in a warming Mediterranean Sea, Biogeosciences,
647 19, 4035-4065, https://doi.org/10.5194/bg-19-4035-2022, 2022.
648 Ribotti, A., Sorgente, R., Pessini, F., Cucco, A., Quattrocchi, G., and Borghini, M.: Twenty-one years of
649 hydrological data acquisition in the Mediterranean Sea: quality, availability, and research, Earth Syst. Sci. Data,
650 14, 4187–4199, https://doi.org/10.5194/essd-14-4187-2022 , 2022.
651 Schroeder, K., Tanhua, T., Bryden, H., Alvarez, M., Chiggiato, J., and Aracri, S.: Mediterranean Sea Ship-based
652 Hydrographic Investigations Program (Med-SHIP), Oceanography, 28, 12–15,
653 https://doi.org/10.5670/oceanog.2015.71 , 2015.
654 Schroeder, K., Kovačević, V., Civitarese, G., Velaoras, D., Álvarez, M., Tanhua, T., Jullio, L., Coppola, L., Bensi,
655 M., Ursella, L., Santinelli, C., Giani, M., Chiggiato, J., Aly-Eldeen, M., Assimakopoulou, G., Bachi, G., Bogner,
656 B., Borghini, M., Cardin, V., Cornec, M., Giannakourou, A., Giannoudi, L., Gogou, A., Golbol, M., Or Hazan, O.,
657 Karthäuser, C., Kralj, M., Krasakopoulou, E., Matić, F., Mihanović, H., Muslim, S., Papadopoulos, V.P., Parinos,
658 C., Paulitschke, A., Pavlidou, A., Pitta, E., Protopapa, M., Rahav, E., Raveh, O., Renieris, P., Reyes-Suarez, N.
659 C., Rousselaki, E., Silverman, J., Souvermezoglou, E., Urbini, L., Zer, C., and Zervoudaki, S.: Seawater physics
660 and chemistry along the Med-SHIP transects in the Mediterranean Sea in 2016, Sci. Data, 11, 52,
661 https://doi.org/10.1038/s41597-023-02835-3, 2024.
662 Schroeder, K.: TAlPro2022 CRUISE REPORT R/V BELGICA Cruise n. 2022/12 (Version 1), Zenodo,
663 https://doi.org/10.5281/zenodo.6918731 , 2022.
664 Tanhua, T., Brown, P. J., and Key, R. M.: CARINA: nutrient data in the Atlantic Ocean, Earth Syst. Sci. Data, 1,
665 7–24, https://doi.org/10.5194/essd-1-7-2009 , 2009.
666 Tanhua, T.: Matlab Toolbox to Perform Secondary Quality Control (2nd QC) on Hydrographic Data, ORNL
667 CDIAC-158, Carbon Dioxide Inf. Anal. Center, Oak Ridge Natl. Lab., U.S. Dep. Energy, Oak Ridge, Tennessee,
668 158, https://doi.org/10.1002/lom3.10050 , 2010.
669 Tanhua, T.: Hydrochemistry of water samples during MedSHIP cruise Talpro, PANGAEA,
670 https://doi.org/10.1594/PANGAEA.902293 , 2019a.
671 Tanhua, T.: Physical oceanography during MedSHIP cruise Talpro [dataset], PANGAEA,
672 https://doi.org/10.1594/PANGAEA.902330 , 2019b.
673 Uchida, H. Johnson, G. C. and McTaggart, G. C.: CTD Oxygen Sensor Calibration Procedures. In, The GO-SHIP
674 Repeat Hydrography Manual: A Collection of Expert Reports and Guidelines. Version 1, (eds Hood, E.M., C.L.
675 Sabine, and B.M. Sloyan), 17pp. (IOCCP Report Number 14; ICPO Publication Series Number 134),
676 https://doi.org/10.25607/OBP-1344, 2010.